Thermodynamic Bounds on Infrared-Modulated ATP Synthesis: Separating Photothermal Heating, Passive Polaritonic Catalysis, and Coherent Ratchets at 71 THz

Lluis Eriksson

Independent Researcher (https://github.com/lluiseriksson)

Bioenergetic Audit Continuing ARR-2025-2AQXS44H6Z8GQAG2 and ARR-2026-1E91AXEJYT890TQC

November 27, 2026

Abstract

In September 2026, Yang, Gu, and Song (bioRxiv:10.64898/2026.09.10.750628v1, unrefereed) reported an approximately 10% increase in cellular ATP levels when living cells are exposed to weak resonant 71/87 THz mid-infrared irradiation, attributing the effect to a mitochondrial cristae polariton. While our companion record ARR-2026-1E91AXEJYT890TQC audited the spectral Hopfield A^2 invariants and coherence-holding horizon, the physical mechanism of the +10% ATP enhancement remained unaudited. Here we establish sharp, machine-checked thermodynamic bounds separating four distinct mechanisms for a +10% steady-state mitochondrial ATP-synthesis flux (J_{ATP}) boost—direct stoichiometric photon-to-ATP conversion, polaritonic catalysis (distinguishing static dark-cavity vacuum ZPE ceilings from irradiance-driven resonant catalysis), micro-hotspot versus bulk photothermal heating, and active coherent ratchets—while noting that cellular ATP concentration ([ATP]) can also rise without mitochondrial flux acceleration via reduced consumption or glycolysis. Backed by a zero-floating-point verification suite (MITO-ATP-MODULATION-CERT-1.0) comprising 20 constructive Lean 4.36.0 integer/rational theorems (0 sorry, 0 grind, 0 Classical.choice, -DwarningAsError=true), 16 SHA-256 canonical certificates (C01–C16), and 58 adversarial pytest checks, five exact results emerge: (i) by the First Law at $\Delta G_{\mathrm{ATP}} = 518.2$ meV and $h \cdot 71$ THz $= 293.63$ meV, stoichiometric conversion requires $2591/1468 \approx 1.765 > 1.76$ absorbed 71-THz photons per extra ATP (tightened strictly by Carnot efficiency $\eta_C = 1 - T/T_{\mathrm{rad}}$); (ii) rational Mercator partial sums $11437/120000 < \ln(11/10) < 143/1500$ pin the Eyring barrier shift at $T = 310$ K to $|\Delta E_a|_{10\%} \in (2.545, 2.547)$ meV; deriving the resonant Hopfield A^2 upper branch $\nu_+ = 7569/71 \approx 106.61$ THz gives single-mode ZPE shift $\Delta E_{\mathrm{ZPE}} = \frac{128}{71}\, h \cdot \mathrm{THz} \approx 7.456$ meV $> 2.92\,|\Delta E_a|_{10\%}$ as an undiluted collective energetic ceiling, while $1/N$ dipole dilution closes static single-enzyme dark catalysis across $N \sim 10^6$–10^8 uncorrelated dipoles and an $I_{\mathrm{inc}} > 0$ flux boost over dark control requires driven resonant catalysis (forcing +10% oligomycin-sensitive ATP-linked OCR under fixed P/O stoichiometry); (iii) exact finite-difference Arrhenius kinetics ($\Delta T_{10\%} \in (1.52, 1.54)$ K at $E_a = 50$ kJ/mol) and steady-state spherical conduction yield a π-free micro-hotspot flux floor $I_{\mathrm{micro}} = 4\kappa_{\mathrm{th}}\Delta T/R > 729$ W/cm^2 (734.4 W/cm^2 at midpoint 1.53 K), excluding single-organelle hotspots under 10 mW/cm^2 mid-IR by $> 72{,}900\times$ while exposing $\geq 2000\times$ bulk dish amplification; (iv) the dimensionally homogeneous Barato–Seifert TUR ($\mathrm{Var}(J_\tau)\,\sigma\tau \geq 2k_B\langle J_\tau\rangle^2$ at explicit window $\tau = 1$ s) bounds classical Markovian NESS catalysis while First-Law additive power conservation ($P_{\mathrm{maint}} + P_{\mathrm{ATP}} \leq P_{\mathrm{in}}$, with $P_{\mathrm{maint}} \sim 5 \times 10^5 P_{\mathrm{ATP}}^{\mathrm{mito}}$) constrains active coherent ratchets; and (v) a four-protocol experimental matrix separates mitochondrial flux acceleration from consumption/glycolytic [ATP] shifts, bulk heating, and stoichiometric conversion.

1 Introduction and Epistemic Scope

In ARR-2025-2AQXS44H6Z8GQAG2 [3], we established an operational thermodynamic pipeline linking membrane geometry to continuous coherence maintenance power. Applying that framework in ARR-2026-1E91AXEJYT890TQC [4] to the unrefereed preprint of Yang, Gu, and Song [7] proved that bulk-water dephasing exceeds the mitochondrial ATP power budget by 5×10^5, cleanly separating passive vacuum-dressed polaritons (Regime I, $C_\Delta = 0$) from active non-equilibrium coherence (Regime II, $C_\Delta > 0$).

A central empirical claim of [7], however, is that weak resonant 71/87 THz irradiation elevates cellular ATP levels by $\sim 10\%$ over dark controls. As in [4], we treat [7] strictly as an unrefereed preprint awaiting independent replication; our goal is to derive exact, machine-checked thermodynamic inequalities distinguishing heating arti-

facts, polaritonic catalysis, stoichiometric photon conversion, and active ratchets.

2 Four Exact Bioenergetic Bounds

2.1 First-Law Stoichiometric and Carnot Photon Floors

At physiological $T = 310$ K, ATP hydrolysis releases $\Delta G_{\mathrm{ATP}} \approx 50$ kJ/mol ≈ 518.2 meV, whereas a single 71 THz photon carries $h\nu_- \approx 293.63$ meV. By the First Law, any direct stoichiometric photon-to-ATP conversion demands (Lean Thm. 1; `C01`–`C04`, Fig. 1a):

$$\frac{\Delta G_{\mathrm{ATP}}}{h\nu_-} = \frac{5182}{2936} = \frac{2591}{1468} \approx 1.765 > \frac{7}{4}\ \mathrm{ph/ATP}, \quad (1)$$

or $\Phi_{71}^{\mathrm{stoich}} > 1.76 \times 10^4$ photons/s/mitochondrion (~ 0.83 fW) for a +10% boost on $J_{\mathrm{ATP}} = 10^5$ ATP/s. Under a finite effective radiation temperature $T_{\mathrm{rad}} > T$ (benchmarked parametrically in `C01`–`C03` at $T_{\mathrm{rad}} = 3100$ K and 620 K; for high-brightness narrowband mid-IR lasers $\eta_C \to 1$), Carnot efficiency $\eta_C = 1 - T/T_{\mathrm{rad}} < 1$ strictly tightens $P_{\mathrm{in}} \geq P_{\mathrm{ATP}}/\eta_C > P_{\mathrm{ATP}}$ whenever $P_{\mathrm{ATP}} > 0$ (Thm. 2).

2.2 Eyring Catalysis, Collective ZPE Ceiling, and Mitochondrial OCR

Under Eyring transition-state kinetics [5] at fixed $T = 310$ K, multiplying turnover rate by 11/10 requires an activation-barrier shift $|\Delta E_a|_{10\%} = k_B T \ln(11/10)$. By the classical alternating-series error bound for the Mercator expansion of $\ln(1+x)$ at $x = 1/10$ (prose calculus; rational partial sums certified over $\mathbb{Z}$ in Lean Thm. 3):

$$\frac{11437}{120000} < \ln\left(\frac{11}{10}\right) < \frac{143}{1500}$$
$$\implies |\Delta E_a|_{10\%} \in (2.545, 2.547)\ \mathrm{meV} \quad (2)$$

at $k_B T = 26.713$ meV (Thm. 4). To benchmark against the resonant Hopfield A^2 polariton energy scale ($\omega_c = \omega_0 = 87$ THz, $\nu_- = 71$ THz, $\eta = g/\omega_0 = 1264/6177 \approx 0.205$ [4]), the TRK invariant $\nu_+\nu_- = \omega_0^2$ fixes the upper polariton at $\nu_+ = 7569/71 \approx 106.61$ THz, giving the exact single-mode ground-state zero-point energy (ZPE) shift (Thm. 5; `C05`–`C08`, Fig. 1b):

$$\Delta E_{\mathrm{ZPE}} = \frac{1}{2}h(\nu_+ + \nu_- - 2\omega_0) = \frac{h(\omega_0 - \nu_-)^2}{2\nu_-}$$
$$= \frac{128}{71}\, h \cdot \mathrm{THz} \approx 7.456\ \mathrm{meV} > 2.92\,|\Delta E_a|_{10\%}. \quad (3)$$

Crucially, (3) and `C05`–`C08` benchmark only the *undiluted collective single-mode ZPE scale* against $|\Delta E_a|_{10\%}$. Two physical obstructions prevent naive static vacuum catalysis from explaining [7]: (a) across $N \sim 10^6$–10^8 uncorrelated lipid dipoles, per-molecule vacuum shifts dilute as $\mathcal{O}(\Delta E_{\mathrm{ZPE}}/N)$, closing static single-enzyme catalysis unless an enzyme reaction coordinate couples coherently to the collective bright mode or a localized few-dipole microdomain; and (b) dark-cavity vacuum ZPE exists already at $I_{\mathrm{inc}} = 0$, so an *irradiance-triggered* +10% boost over a dark control ($I_{\mathrm{inc}} > 0$ vs. 0) requires *irradiance-driven resonant polaritonic catalysis* (weak resonant 71-THz excitation of MP^- carrying $h\nu_- = 293.63$ meV per quantum, saturating sub-linearly as $I_{\mathrm{inc}}/(I_{\mathrm{inc}} + I_{\mathrm{sat}})$ at high irradiance, Thm. 20).

Flux vs. cellular abundance distinction. Importantly, cellular ATP concentration ([ATP]) reported in [7] can rise without accelerating oxidative phosphorylation if cellular ATP consumption drops, glycolysis compensates, or ATP synthase operates near equilibrium under fixed demand. Conditional on the hypothesis that the +10% increase reflects a +10% boost in *steady-state mitochondrial ATP-synthesis flux* J_{ATP} under Mitchell's chemiosmotic coupling [6] with fixed H^+/ATP and P/O stoichiometry, catalytic acceleration leaves the coupled P/O ratio invariant (Thm. 19) and forces an exact +10% increase in *oligomycin-sensitive ATP-linked OCR* (Thm. 13). For antimycin/rotenone-corrected mitochondrial OCR ($J_{\mathrm{mito}} = J_{\mathrm{ATP\text{-}linked}} + J_{\mathrm{leak}}$), whenever proton leak stays fixed at $\leq 25\%$, total mitochondrial OCR rises by $\geq +7.5\%$ (Thm. 17; non-ohmic proton leak may decrease modestly if Δp drops slightly under faster ATP synthesis). Conversely, observing a +10% [ATP] rise with *zero* oligomycin-sensitive OCR increase immediately separates reduced ATP demand, glycolytic shift, or direct non-O_2 work from mitochondrial oxidative catalysis. Under CCCP/FCCP uncoupling ($\Delta p \to 0$), forward chemiosmotic ATP synthesis vanishes (and F_1F_o-ATPase typically reverses to hydrolyze ATP, eliminating any forward catalytic synthesis gain, Thm. 16).

2.3 Exact Finite-Difference Arrhenius and π-Free Micro-Hotspot No-Go

Under Arrhenius heating (incorporating the Eyring T prefactor reduces $\Delta T_{10\%}$ by $\sim 5\%$ to ~ 1.45 K, leaving the micro-hotspot exclusion $> 69{,}000\times$ unchanged), a +10% rate jump obeys the exact finite-difference identity (Thm. 6; zero linearization error):

$$\frac{E_a}{k_B T} - \frac{E_a}{k_B(T + \Delta T)} = \ln\left(\frac{11}{10}\right)$$
$$\iff \Delta T_{10\%} = \frac{T\,\Delta E_a}{E_a - \Delta E_a}. \quad (4)$$

With (2) at $T = 310$ K, respiratory activation energy $E_a = 50$ kJ/mol (518.2 meV) forces $\Delta T_{10\%} \in (1.52, 1.54)$ K (> 1.90 K at 40 kJ/mol, > 1.26 K at 60 kJ/mol, Thm. 7, Fig. 2a).

By the steady-state spherical heat equation [1], sustaining ΔT across a mitochondrion of radius $R = 0.5$ μm in aqueous cytosol ($\kappa_{\mathrm{th}} = 3/5$ W/(m · K)) requires absorbed power $P_{\mathrm{micro}} = 4\pi\kappa_{\mathrm{th}} R \Delta T > 5.7$ μW (nearly $10^{10}\times$ the

0.83 fW stoichiometric floor, Thm. 9). Dividing by cross-section $A = \pi R^2$ cancels π identically (Thm. 8):

$$I_{\text{micro}} = \frac{P_{\text{micro}}}{\pi R^2} = \frac{4\kappa_{\text{th}}\Delta T}{R} = 734.4\ \text{W/cm}^2\ \ (1.53\ \text{K}), \quad > 729.6\ \text{W/cm}^2\ \ (1.52\ \text{K}) \tag{5}$$

Since absorbed flux satisfies $I_{\text{abs}} \leq I_{\text{inc}}$ (even at 100% single-organelle absorption), weak mid-IR irradiation ($I_{\text{inc}} \leq 10$ mW/cm^2 = 100 W/m^2) falls short of single-organelle micro-thermal heating by $> 72{,}900\times$ ($> 73{,}400\times$ at midpoint 1.53 K, Thm. 10; `C09`–`C12`, Fig. 2b), and basal respiratory self-heating stays below 10^{-8} K (Thm. 12). By contrast, collective heating across a 1 mm culture dish amplifies ΔT by at least $L/R = 2000\times$ in 3D spherical scaling (Thm. 11, down to ~ 0.37 W/cm^2)—and further under 1D planar substrate thermal resistance or cm-scale illumination—making an off-resonance water-absorption-matched IR control the primary discriminator separating bulk heating (H_{bulk}) from weak-field resonant catalysis (H_{cat}).

2.4 Classical Markovian TUR (Window $\tau = 1$ s) and Ratchet Power Floor

For *autonomous classical Markovian non-equilibrium steady states* observed over an explicit time window τ (overdamped biochemical catalysis, `C13`–`C16` evaluated at $\tau = 1$ s, Fig. 3a), integrated ATP-flux precision obeys the dimensionally homogeneous Barato–Seifert thermodynamic uncertainty relation [2]:

$$\frac{\text{Var}(J_\tau)}{\langle J_\tau \rangle^2} \frac{\sigma\tau}{k_B} \geq 2 \qquad (\sigma \geq 0,\ \tau > 0), \tag{6}$$

where $\sigma\tau/k_B$ is strictly dimensionless (with $\sigma_\tau := \sigma\tau$ replacing σ in the cleared integer implication of Lean Thm. 14; `C13`–`C14` use illustrative $\text{Var}(J_\tau)/\langle J_\tau \rangle^2 = 10^{-2}, 10^{-3}$). Classical periodically driven ratchets ($C_\Delta = 0$) can bypass the autonomous TUR without incurring quantum coherence-maintenance costs and remain constrained by First-Law power balance $P_{\text{ATP}} + P_{\text{loss}} = P_{\text{in}}$ (Thm. 15). By contrast, an *active Regime II quantum-coherent ratchet* ($C_\Delta > 0$) must satisfy the exact additive power floor $P_{\text{maint}} + P_{\text{ATP}} \leq P_{\text{in}}$ (Thm. 15): taking the bulk-water dephasing maintenance estimate $P_{\text{maint}} \sim 5 \times 10^5\, P_{\text{ATP}}^{\text{mito}} \sim 4$ nW per mitochondrion from [4], this exceeds the total weak mid-IR power incident on a single mitochondrion ($I_{\text{inc}}\pi R^2 \approx 78.5$ pW at 10 mW/cm^2, $R = 0.5\ \mu$m) by $> 50\times$ even at 100% absorption.

3 Formal Certification Scope and Reproducibility

Exact verification boundary. Layer 1 (`src/lean/MitoAtpModulationCert.lean`, 20 constructive integer/rational theorems compiled under Lean 4.36.0 `-DwarningAsError=true`, `0 sorry`, `0 grind`, `0 Classical.choice`, Table 1) certifies the exact rational partial-sum, TRK-to-ZPE, Arrhenius, π-free flux, OCR, TUR-implication, and additive power-balance inequalities over $\mathbb{Z}$. Layer 2 (`src/python/mito_atp_modulation_verifier.py`, AST-audited zero-float, zero `/`, zero `**`, zero `limit_denominator`) verifies all 16 SHA-256 certificates (`C01`–`C16`, Table 2, archived in `data/certificates/MANIFEST.json`) and passes all 58 adversarial checks. Analytical series-remainder bounds ($\ln(11/10)$), continuum conduction, chemiosmotic kinetics, classical TUR applicability, and unrefereed empirical inputs from [7] reside in prose and Table 3 rather than inside the Lean kernel.

AI Assistance Disclosure. Authored by Lluis Eriksson with Google Antigravity assisting Lean 4 proof engineering, zero-float verifier implementation, adversarial testing, 300-DPI figures, and LaTeX drafting. All Lean 4 proofs (`src/lean/`), zero-float verifier (`src/python/`), and 16 JSON certificates (`data/certificates/`) are archived directly in this public AIRR record under MIT (code/Lean/data) and CC-BY-4.0 (manuscript/figures).

References

[1] Guillaume Baffou, Hervé Rigneault, Didier Marguet, and Ludovic Jullien. A critique of methods for temperature imaging in single cells. *Nature Methods*, 11:899–901, 2014.

[2] Andre C. Barato and Udo Seifert. Thermodynamic uncertainty relation for biomolecular processes. *Physical Review Letters*, 114:158101, 2015.

[3] Lluis Eriksson. Geometry, membranes, and life as a resource boundary: A correct-by-construction operational pipeline from static suppression to maintenance costs. 2025. AIRR.SCIENCE record ARR-2025-2AQXS44H6Z8GQAG2 (ai.viXra:2512.0085, v1 Dec 2025; v2 Jul 2026).

[4] Lluis Eriksson. Mito-polaritons meet the resource boundary: Exact Hopfield A^2 invariants, thermodynamic maintenance horizons, and constructive Lean 4 certificates for the 71-THz mitochondrial quantum state. 2026. AIRR.SCIENCE record ARR-2026-1E91AXEJYT890TQC (accepted Nov 26, 2026).

[5] Henry Eyring. The activated complex in chemical reactions. *Journal of Chemical Physics*, 3:107–115, 1935.

[6] Peter Mitchell. Coupling of phosphorylation to electron and hydrogen transfer by a chemi-osmotic type of mechanism. *Nature*, 191:144–148, 1961.

[7] Yu Yang, Zhenglong Gu, and Bo Song. A quantum state of mitochondria in the living cell. 2026. bioRxiv preprint 10.64898/2026.09.10.750628v1, 15 September 2026 (unrefereed).

Table 1: All 20 constructive Lean 4.36.0 theorems in `src/lean/MitoAtpModulationCert.lean` (`0 sorry`, `0 grind`, `0 Classical.choice`, `-DwarningAsError=true`).

#	Lean Theorem Identifier	Exact Formalized Statement (over $\mathbb{Z}$)
1	`first_law_stoichiometric_photon_floor`	$5182/2936 = 2591/1468 \in (1.76, 2)$ ($> 7/4$ photons/ATP)
2	`carnot_tightening_stoichiometric_power`	$0 < P_{\mathrm{ATP}} \wedge 0 < T < T_{\mathrm{rad}} \wedge P_{\mathrm{ATP}} T_{\mathrm{rad}} \le P_{\mathrm{in}}(T_{\mathrm{rad}} - T) \implies P_{\mathrm{ATP}} < P_{\mathrm{in}}$
3	`exact_mercator_ln_11_10_bracket`	$953/10000 < 11437/120000 < 143/1500 < 954/10000$ (Mercator partial sums)
4	`eyring_passive_catalytic_barrier_310k`	$2545 < 26713 \cdot (11437/120000)$ and $26713 \cdot (143/1500) < 2547$ (μeV)
5	`hopfield_zpe_exceeds_catalytic_barrier_2p9x`	$\nu_+\nu_- = \omega_0^2 \implies \nu_-(\nu_+ + \nu_- - 2\omega_0) = (\omega_0 - \nu_-)^2$; $\Delta E_{\mathrm{ZPE}} \in (7.455, 7.457)$ meV
6	`exact_finite_difference_arrhenius_identity`	$E_a\,\Delta T = L\,k_B T(T + \Delta T) \implies (E_a - Lk_BT)\Delta T = Lk_BT^2$
7	`arrhenius_delta_t_brackets_310k`	$\Delta T_{10\%} \in (1.52, 1.54)$ K (50 kJ/mol), > 1.90 K (40), > 1.26 K (60)
8	`pi_free_micro_hotspot_flux_nogo`	$I_{\mathrm{micro}} R = 4\kappa_{\mathrm{th}}\Delta T$; $I_{\mathrm{micro}} = 7344000$ W/m^2 > 734 W/cm^2 (1.53 K)
9	`micro_hotspot_vs_stoichiometric_power_gap`	$P_{\mathrm{micro}} > 5.7\ \mu\mathrm{W} > 5 \times 10^9$ fW vs. $P_{\mathrm{stoich}} < 1$ fW
10	`weak_ir_micro_hotspot_exclusion`	$0 < I_{\mathrm{inc}} \le 100$ W/m$^2 \implies 73400\, I_{\mathrm{inc}} < 7344000$ ($> 73400\times$ at 1.53 K)
11	`bulk_vs_micro_thermal_length_amplification`	$L/R \ge 2000$ (1 mm dish vs. 0.5 μm organelle)
12	`basal_mitochondrion_self_heating_negligible`	$20000 < 4 \cdot 314 \cdot 6 \cdot 5$ ($\Delta T_{\mathrm{basal}} < 10^{-8}$ K)
13	`catalytic_ocr_proportionality_law`	Fixed ATP-linked stoichiometry $\wedge\ 10\,\Delta J_{\mathrm{ATP}} = J_{\mathrm{ATP}} \implies 10\,\Delta J_{\mathrm{O_2}} = J_{\mathrm{O_2}}$
14	`barato_seifert_tur_entropy_floor`	$e_D > 0 \wedge \sigma_\tau \ge 0 \wedge 2k_BJ^2 \le \mathrm{Var} \cdot \sigma_\tau \wedge \mathrm{Var} \cdot e_D \le e_N J^2 \implies 2k_BJ^2 e_D \le e_N J^2 \sigma_\tau$
15	`active_coherent_ratchet_dual_floor`	$P_{\mathrm{maint}}, P_{\mathrm{ATP}}, P_{\mathrm{loss}} \ge 0 \wedge P_{\mathrm{maint}} + P_{\mathrm{ATP}} + P_{\mathrm{loss}} = P_{\mathrm{in}} \implies P_{\mathrm{maint}} + P_{\mathrm{ATP}} \le P_{\mathrm{in}}$
16	`uncoupler_collapses_passive_catalysis`	$\Delta p = 0 \implies (11k_{\mathrm{cat}}) \cdot 0 = (10k_{\mathrm{cat}}) \cdot 0 = 0$ (CCCP collapse)
17	`proton_leak_adjusted_ocr_lower_bound`	$J_{\mathrm{mito}} = J_c + J_{\mathrm{leak}} \wedge 4J_{\mathrm{leak}} \le J_{\mathrm{mito}} \wedge 10\Delta J = J_c \implies 40\Delta J \ge 3J_{\mathrm{mito}}$ ($\ge +7.5\%$)
18	`atp_mechanism_discriminator_decidability`	Joint numerical check: > 1.76 ph/ATP, $> 2.92\times$ ZPE scale, $> 73400\times$ micro, $2000\times$ bulk
19	`catalytic_po_ratio_invariance`	$2(\mathrm{P/O})J_{\mathrm{O_2}} = J_{\mathrm{ATP}} \implies 2(\mathrm{P/O})(11J_{\mathrm{O_2}}) = 11J_{\mathrm{ATP}}$
20	`catalytic_saturation_strict_ceiling`	$A, I_{\mathrm{sat}} > 0 \wedge I \ge 0 \implies AI < A(I + I_{\mathrm{sat}})$ (sub-linear saturation ceiling)

Table 2: Summary of all 16 verified `MITO-ATP-MODULATION-CERT-1.0` canonical certificates (`C01`–`C16`, SHA-256 hashed in `data/certificates/MANIFEST.json`).

ID	Mode	Verified Instance	Exact Certified Metrics
`C01`	M1 Stoich/Carnot	71 THz, $\Delta G = 518.2$ meV, $T_r = 3100$ K	$2591/1468 \approx 1.765$ ph/ATP (1st Law), 1.961 (Carnot $\eta_C = 9/10$)
`C02`	M1 Stoich/Carnot	87 THz, $\Delta G = 518.2$ meV	1.440 ph/ATP (1st Law), 1.600 ph/ATP (Carnot)
`C03`	M1 Stoich/Carnot	71 THz, $T_r = 620$ K ($\eta_C = 1/2$)	3.530 ph/ATP (exact $2\times$ Carnot tightening)
`C04`	M1 Stoich/Carnot	71 THz, $\Delta G = 621.8$ meV (60 kJ/mol)	2.118 ph/ATP (> 2.1 photons/ATP)
`C05`	M2 ZPE Ceiling	71/87 THz ($\eta \approx 0.205$), +10%	$\lvert\Delta E_a\rvert \in (2.545, 2.547)$ meV, ZPE/$\lvert\Delta E_a\rvert > 2.92\times$ ($1/N$ dil.)
`C06`	M2 ZPE Ceiling	71/87 THz, +25% ATP, 310 K	$\lvert\Delta E_a\rvert \approx 5.96$ meV, collective ZPE/$\lvert\Delta E_a\rvert > 1.25\times$
`C07`	M2 ZPE Ceiling	79/87 THz ($\eta \approx 0.097$), +10%	ZPE = 1.675 meV < 2.55 meV (ratio ≈ 0.66, below barrier)
`C08`	M2 ZPE Ceiling	65/87 THz ($\eta \approx 0.296$), +10%	Deep USC ZPE = 15.4 meV, collective ratio $> 6.0\times$
`C09`	M3 Photothermal	$E_a = 50$ kJ/mol, $I = 10$ mW/cm^2	$\Delta T \in (1.52, 1.54)$ K, $I_{\mathrm{micro}} > 729$ W/cm^2 ($> 72{,}900\times$ excl.)
`C10`	M3 Photothermal	$E_a = 40$ kJ/mol, $I = 10$ mW/cm^2	$\Delta T > 1.90$ K (1.91 K), excluded by $> 91{,}000\times$
`C11`	M3 Photothermal	$E_a = 60$ kJ/mol, $I = 10$ mW/cm^2	$\Delta T > 1.26$ K (1.274 K), excluded by $> 60{,}400\times$ ($61{,}176\times$ exact)
`C12`	M3 Photothermal	$E_a = 50$ kJ/mol, $I = 1$ W/cm^2	Even at 1 W/cm^2, micro-hotspot excluded by $> 729\times$
`C13`	M4 Classical TUR	NADH (P/O = 5/2), $\sigma\tau/k_B = 2 \times 10^6$ ($\tau = 1$ s)	Classical TUR sat. ($2 \times 10^4 \ge 2$), ATP-linked ΔOCR = +10%
`C14`	M4 Classical TUR	$FADH_2$ (P/O = 3/2), $\sigma\tau/k_B = 1.2 \times 10^6$ ($\tau = 1$ s)	Classical TUR sat. ($1200 \ge 2$), P/O = 3/2 invariant
`C15`	M4 TUR Control	Synth. $\sigma\tau/k_B = 10^3$ ($\tau = 1$ s), $\mathrm{Var}/J^2 = 10^{-6}$	$(\mathrm{Var}/J^2)(\sigma\tau/k_B) = 10^{-3} < 2$ (classical TUR viol.)
`C16`	M4 TUR Boundary	Exact sat. $\sigma\tau/k_B = 2 \times 10^5$ ($\tau = 1$ s), 10^{-5}	$(\mathrm{Var}/J^2)(\sigma\tau/k_B) = 2$ exact classical TUR boundary

Table 3: Four-protocol experimental discriminator separating mechanisms for a +10% steady-state mitochondrial ATP-flux (J_{ATP}) increase under 71-THz IR (off-resonance water-matched IR is the primary separator between H_{bulk} and H_{cat}; empirical I_{sat} is not derived from first principles).

Protocol	H_{bulk} (Bulk Heat)	H_{micro} (Hotspot)	H_{cat} (Driven VSC Catalysis)	H_{stoich} (Direct Photon/Ratchet)
Off-res. H_2O-matched IR	+10% ATP	Excluded	0% (sharp 71 THz)	0% (off-res.)
Oligomycin-sens. ATP-OCR	+10% (Arrh.)	Excluded	+10% (if flux-driven; 0% if demand)	$\approx 0\%$ (no extra O_2)
CCCP / FCCP ($\Delta p \to 0$)	Collapses fwd. syn.	Excluded	Collapses fwd. syn. (Thm. 16)	Persists only if direct (non-Δp)
Irradiance sweep (auxiliary)	Linear (below harm)	Excluded	Linear $\ll I_{\mathrm{sat}}$; saturates $\gtrsim I_{\mathrm{sat}}$	Linear below absorber/enzyme sat.

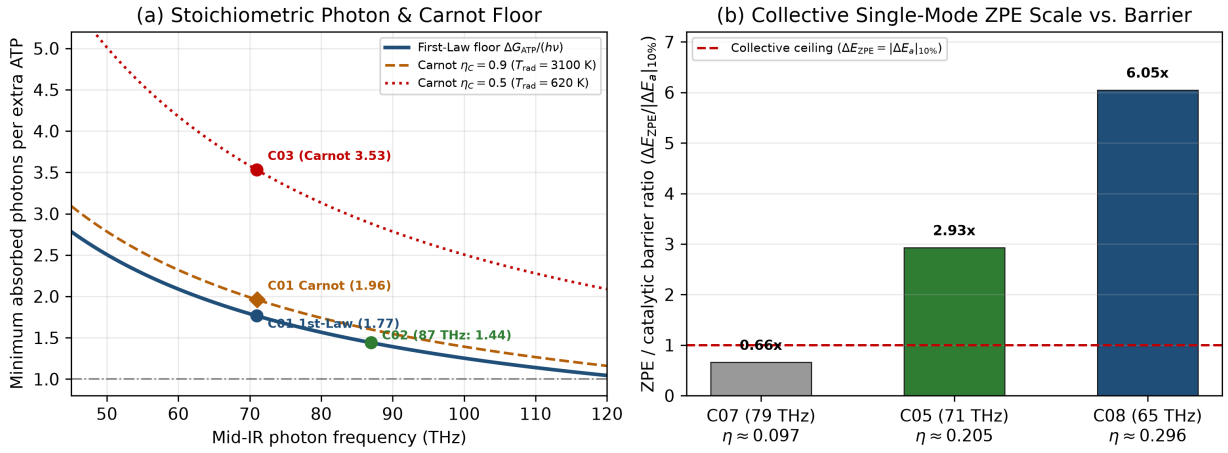

Figure 1: **Stoichiometric Photon Floor and Collective Single-Mode ZPE Scale.** (a) First-Law and Carnot-tightened photons per extra ATP vs. mid-IR frequency (`C01`–`C03`, showing both First-Law 1.77 and Carnot 1.96 for `C01`). (b) Undiluted single-mode Hopfield ZPE-to-catalytic-barrier ratio across normalized coupling $\eta = g/\omega_0$ (`C07`: $\eta \approx 0.097$, 0.66×; `C05`: $\eta \approx 0.205$, 2.93×; `C08`: $\eta \approx 0.296$, 6.05×), representing a collective energetic ceiling subject to $1/N$ dipole dilution.

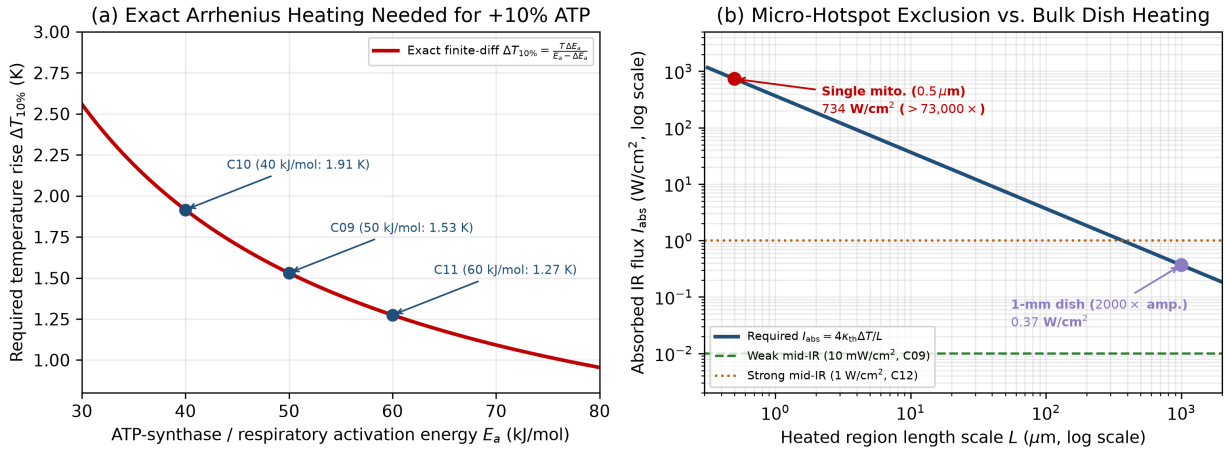

Figure 2: **Photothermal Micro-Hotspot Exclusion vs. Bulk Dish Heating.** (a) Exact finite-difference Arrhenius $\Delta T_{10\%}$ vs. activation energy E_a (`C09`–`C11`). (b) π-free absorbed flux law $I_{\text{abs}} = 4\kappa_{\text{th}}\Delta T/L$ ($I_{\text{abs}} \leq I_{\text{inc}}$) excluding single-mitochondrion hotspots (> 729 W/cm^2, 734.4 W/cm^2 at midpoint) by $> 72{,}900\times$ at 10 mW/cm^2 while exposing $\geq 2000\times$ bulk dish amplification.

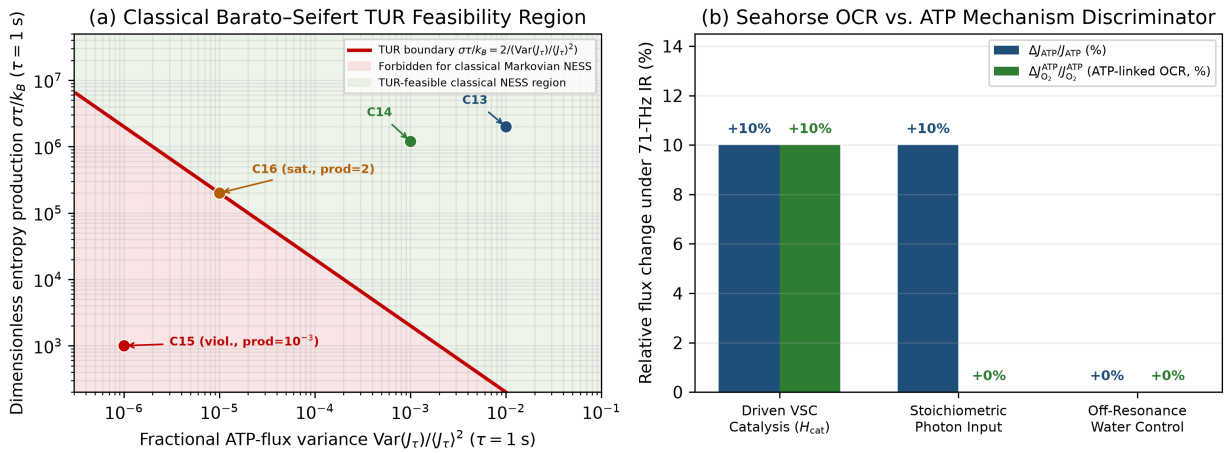

Figure 3: **Classical Markovian TUR Region ($\tau = 1$ s) and Experimental ATP-Linked OCR Discriminator.** (a) Dimensionally homogeneous classical NESS TUR boundary ($\sigma\tau/k_B = 2/(\mathrm{Var}(J_\tau)/\langle J_\tau\rangle^2)$ at $\tau = 1$ s) with illustrative points (`C13`, `C14`), exact saturation (`C16`, product 2), and synthetic violation control (`C15`, product 10^{-3}). (b) Conditional on +10% mitochondrial J_{ATP}, sharp +10% oligomycin-sensitive ATP-linked OCR vs. 0% signature separates driven polaritonic catalysis (H_{cat}) from direct stoichiometric conversion (or reduced-demand/glycolytic [ATP] shifts).